Thermographic Techniques to Explore Small-Scale Processes at Water Surfaces

Bernd Jähne[1,2], Lucas Warmuth[1], Roman Stewing[1], and Kerstin E. Krall[1]

[1] Heidelberg University, Institute for Environmental Physics
Im Neuenheimer Feld 229, 69120 Heidelberg
[2] Heidelberg University, Interdisciplinary Center for Scientific Computing
Berliner Straße 43, 69120 Heidelberg

Abstract Techniques based on thermography are well-established for destruction-free material inspection. A similar technique was invented independently in environmental sciences to explore exchange processes at air-water interfaces. The analysis was, however, limited to one-dimensional vertical transport assuming a horizontally homogeneous and stationary exchange process on average. In this contribution, first steps pursuing a true spatio-temporal approach are presented. This allows much faster measurements, identification of the transport mechanisms and has the prospect to even measure the shear stress right at the water surface, which drives exchange processes at a windy water surface.

Keywords Thermography, Lock-In Technique, Heat Transport, Interface

1 Introduction

Lock-in thermography and heat flux thermography are well-established techniques for destruction-free material inspection [1, 2]. A periodically varying or flashed heat flux is applied at the surface of an object and the temperature response of the surface is captured with a thermographic camera. The applied heat at the surface diffuses into the material of the object. Above cracks, holes or other material inhomogeneities with lower heat conduction, the material surface remains warmer. In this way, it is possible to look below the surface of opaque materials.

It is less known that similar techniques were invented independently in environmental sciences [3,4] to explore exchange processes on ocean, lake, and river surfaces or in laboratory simulation facilities such as wind-wave tunnels. Water would be a perfectly homogeneous material without any flow, because the applied heat at the water surface just diffuses into the bulk of the water body. In reality, turbulent transport processes cause inhomogeneous heat flow at the surface.

Section 2 briefly explains the basics of thermography to explore turbulent transport processes across the air-water interface and the established technique with periodic heating. Then, two new approaches are discussed: a direct analysis of the intermittent transport process under spatially constant irradiation (Section 3) and a line-shaped irradiation to measure the water surface velocity and the gradient of the shear flow (Section 4).

2 Basics

The basic characteristic of transport processes across interfaces is that turbulent transport becomes less efficient closer to the interface because turbulent fluctuations ("eddies") become smaller in size. Below a certain scale, turbulent fluctuations are even damped by viscosity. This leads to the formation of a viscous boundary layer. Therefore, the final transport to the interface can only take place by molecular diffusion.

This basic characteristic of the transport process can be seen in thermographic images, taken after a constant heat flux density was applied to the interface for a certain time. This can be done, for instance, by irradiating the water surface using a CO_2 laser beam expanded to an area of up to a square meter. The radiation penetrates only 14 µm into the water. That means that the controllable heat flux density is placed directly at the surface. An MWIR thermal camera images the water surface temperature over a slightly deeper layer [5]. The 10.6 µm laser radiation is not directly detected in the surface temperature images, because the camera is sensitive only in the 3–5 µm wavelength region.

After 0.5 s, at a low turbulence level with a wind speed of 2 m/s, the heat has penetrated only such a short distance into the water, that it is

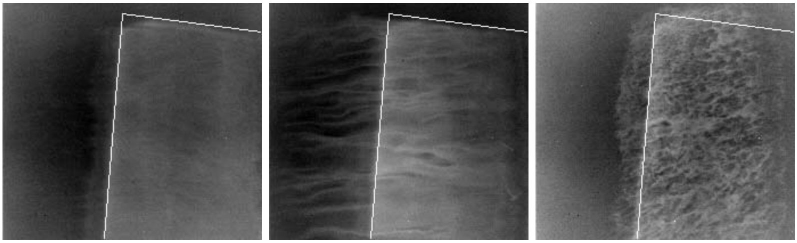

Figure 1: Temperature increase at the water surface in the Heidelberg Aeolotron wind-wave tank. The area heated by a CO_2 laser (about 25 cm $\times$ 25 cm) is marked by white outline. The time after switching on the laser and the wind speed applied to the water surace is given below the images.

still inside the viscous boundary layer. Because heat conduction into the water is driven only by molecular diffusion, the surface temperature in the heated area is uniform (Figure 1, left image). After a four times longer time span (2 s, Figure 1, middle image), the heat has penetrated about twice the distance into the water. Now the influence of the turbulent heat transport in deeper layers starts to become visible. At a higher turbulence level with a wind speed of 7 m/s, the turbulent structures can already be seen 0.5 s after switching on the heat flux and exhibit a much finer scale and different patterns (Figure 1, right image). With a higher wind speed, the induced velocity gradient at the water surface is steeper and turbulence comes closer to the interface.

Previous research of the controlled flux technique has not looked into the evolution of these structures, but rather used it for fast measurements of the speed of heat exchange, expressed by the *transfer velocity* k (units m/s), in wind-wave facilities [6] and at sea [7]. This is because heat can be used as a proxy tracer for environment- and climate-relevant trace gases exchanging across the atmosphere-ocean interface with this technique. All other field measuring techniques integrate and average over much larger spatial and temporal scales [5]. By considering the different diffusion coefficients of heat and gases dissolved in water, the transfer velocity of gases can be computed from those for heat [8].

The periodic variation of the heat flux by a CO_2 laser — or lock-in technique — has the advantage that all the information about the response of the system is contained in the switching frequencies and its higher harmonics. Constant or randomly fluctuating heat flux densities by sensible heat transfer, latent heat transfer (evaporation) or radiative cooling into the sky, are the more suppressed, the longer the amplitude variation is measured.

At low switching frequencies, the heat response at the surface can follow the applied heat flux density j and reaches a constant temperature increase of

$$\Delta T = \frac{j}{\rho c_p k} \quad \rightsquigarrow \quad k = \frac{j}{\rho c_p \Delta T}, \tag{1}$$

so that k can be determined if the heat flux density is known; ρ is the density and c_p the specific heat capacity of water. If the switching frequencies are increased beyond a critical frequency ν_c, the amplitude of the temperature response starts to decrease. Finally, the penetration depth becomes so shallow that the response is no longer determined by turbulence but only by molecular diffusion. Then the temperature amplitude response ΔT is given by [4]

$$\Delta T = \frac{j}{\rho c_p (2\pi \nu D_h)^{1/2}}. \tag{2}$$

D_h is the molecular diffusion coefficient for heat in water (thermal diffusivity). The frequency response is therefore similar to a low-pass filter. However, the amplitude response for higher frequencies does not decrease with ν^{-1} but slower, only with $\nu^{-1/2}$. The asymptotic constant and the damped parts of the amplitude response curve meet at the critical frequency ν_c (Figure 2). Eqs. (1) and (2) yield

$$\nu_c = \frac{k^2}{2\pi D_h} \quad \rightsquigarrow \quad k = \sqrt{2\pi \nu_c D_h}. \tag{3}$$

This means that the transfer velocity k can also be computed from the measurement of the amplitude response without any knowledge about the heat flux density j. Figure 2 also shows that transport across the thin heat boundary layer at the water surface is quite fast. Up to frequencies of 1 Hz the amplitude response shows no damping.

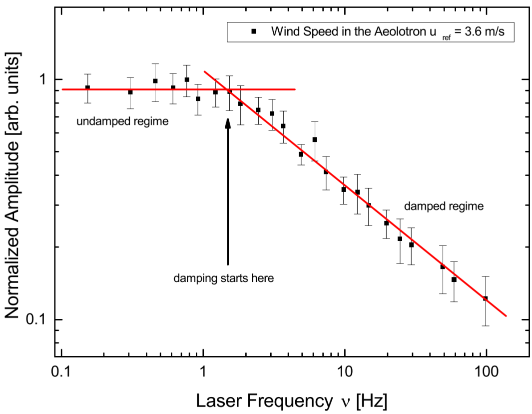

Figure 2: Frequency response of the heat boundary layer at the water surface for frequencies between 0.1 to 100 Hz; from [9].

3 Analysis of intermittency

The approach discussed so far has still two deficits. Firstly, the measurements are still quite slow, because averaging over several periods of the periodic heating and a frequency sweep are required. Secondly, horizontal averaging over the heated footprint is performed. The averaging over both temporal and spatial scales misses all the important information contained in the patterns.

In this paper, two first steps into a true spatio-temporal analysis are described. The setup used for these measurements is shown in Figure 3. At the water surface, the camera images an area larger than the area heated by the CO_2 laser. Because of the drift of the water induced by the wind, a characteristic temperature profile averaged perpendicular to the wind direction and time establishes (red line in Figure 4). There is a heating zone characterized by an increase in temperature followed by an equilibrium zone with more or less constant temperature. After the water leaves the heated zone, the mean temperature decays again.

The analysis here is limited to the equilibrium zone averaged only over 25 images taken with a frame rate of 600 Hz. This arrangement

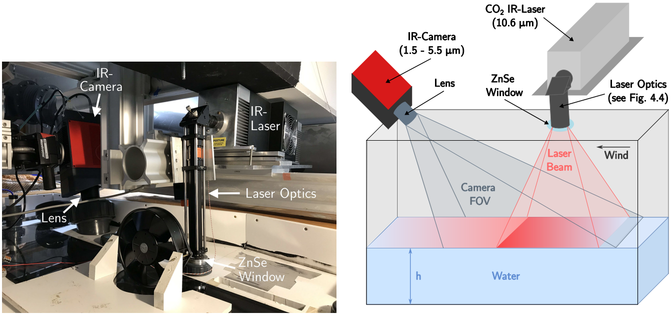

Figure 3: Setup of thermography at the ceiling of the Heidelberg Aeolotron; from [10]

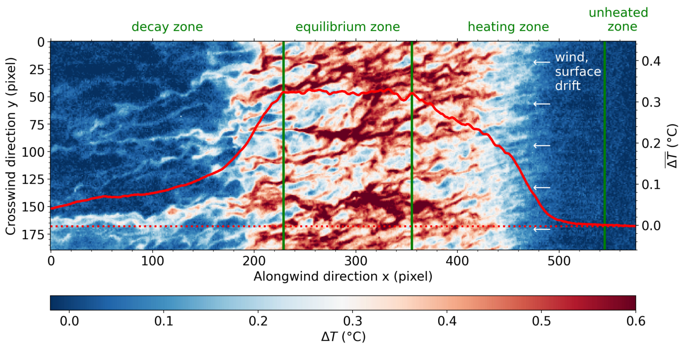

Figure 4: Temperature response at water surface by heating an area of about 60 cm × 60 cm. Wind direction is right to left; from [10].

made it possible to measure the transfer velocity instantaneously according to Eq. (1) with a temporal resolution of 0.042 s. This is faster than the time constant of the transfer process.

A few seconds after the measurements were started, the wind was switched on and within several seconds the transfer velocity jumped up (Figure 5). At the lowest wind speed, the transfer velocity remains quite constant, whereas with increasing wind speed more and more spikes with up to 10 times higher transfer velocity show up. They could be related to extensive turbulent mixing at the surface caused by micro–scale wave breaking events (wave breaking without bubble en-

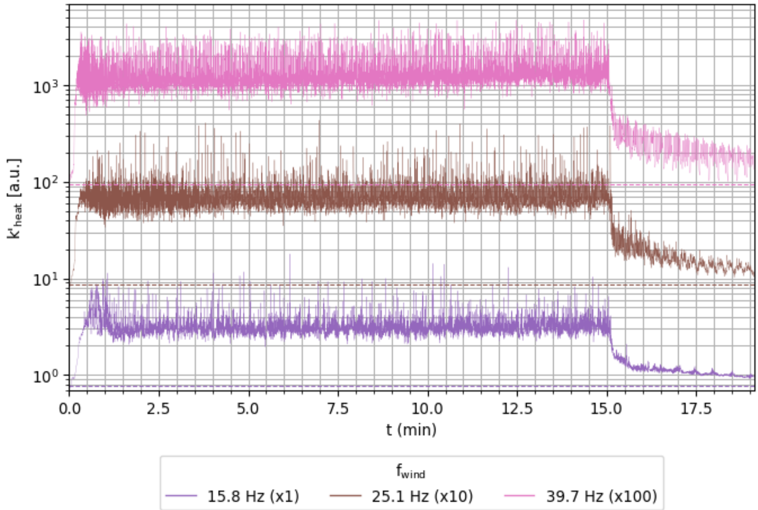

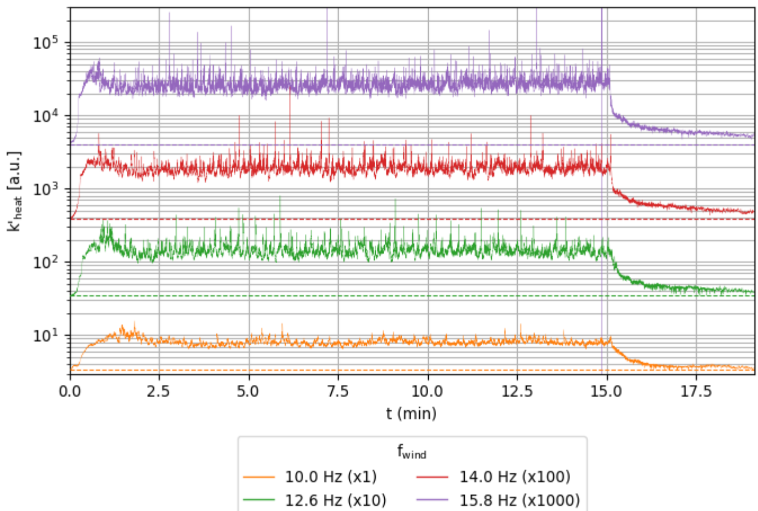

Figure 5: Instantaneous transfer velocities k measured at different wind speeds (indicated by the drive frequency of the wind fans) in the Heidelberg Aeolotron with a water depth of 32 cm. The wind was switched on a few seconds after the start of the measurement and was kept on for 15 min; from [10].

trainment). After the start of the wind, the wind-wave field gradually evolves from small ripples to larger and larger gravity waves. Except for the initial waves at medium wind speeds, where a clear overshoot of the transfer velocity is observed, the transfer velocity is remarkably insensitive to status of the wind wave field. When the wind is stopped after 15 min, the transfer velocity immediately decreases.

4 Analysis of the shear current at the interface

The measurements shown above, clearly demonstrate that the wind is the main driver of the transport process. The wind induces a shear flow at the water interface within the aqueous viscous boundary layer. This shear layer can also be investigated using thermography. The key idea is to heat up only a line perpendicular to the wind direction at the water surface with a penetration depth for the radiation of about one millimeter matching the thickness of the viscous mass boundary and to apply a short pulse of a few milliseconds, which yields a very thin heated line. If only the surface was heated up by a CO_2 laser, the line would quickly disappear because of vertical diffusion into the water. With the deeper penetration depth used here, vertical diffusion is not dominant so that the horizontal transport in the shear layer can be studied. An Erbium fiber laser with a wavelength in the near infrared (1568 nm) is used, which has a penetration depth of 1.0 mm.

Stewing [11] showed that the widening of the lines at the water surface is proportional with the diffusion of heat in horizontal direction, as long as there is no shear current at the water surface, but only the water body as a whole moves in the water channel of a wind-wave facility (Figure 6, lower left image). This is already the case a few seconds after the wind is turned off. Because of inertia, the water body continues to move and decreases its velocity only slowly [12].

With a wind-induced shear current at the water surface, the situation is completely different (Figure 6, first three images). Because of the velocity gradient at the water surface, different parts of the heated line move with different velocities. Although only the heated line at the water surface is seen, the slower moving parts now diffuse also vertically towards the surface. The result is that the line widens much faster in flow direction and its temperature drops much faster. The complexity

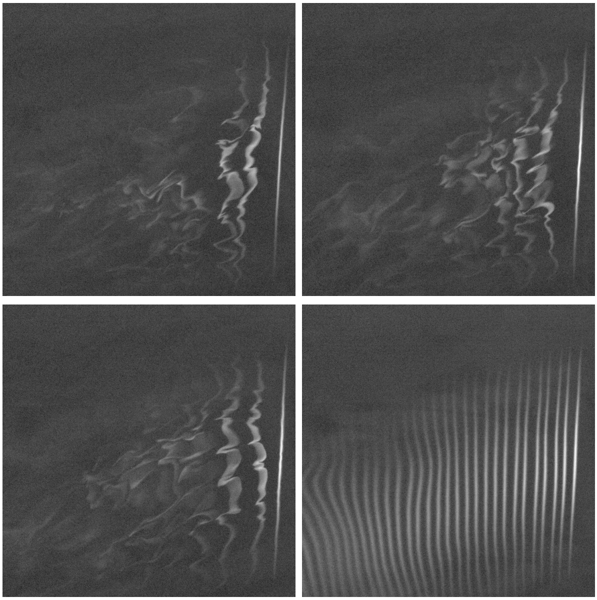

Figure 6: Evolution of heated lines produced by a 100 W 1540 nm fiber laser with 10 ms duration every 200 ms at a low wind speed in the Heidelberg Aeolotron; lower left thermal image seconds after the wind has been turned off; image sector about 20 cm $\times$ 20 cm.

of the velocity field at the water surface influenced by a wind-induced shear current together with wind-induced waves can be seen and studied in these images. The flow field at the surface is turbulent and there are thin streaks in wind direction with much higher velocity.

5 Conclusions and outlook

The active thermography techniques described here show how powerful this optical inspection methods are. They allow a detailed analysis of complex flow fields and transport processes at free interfaces and can look below the surface. This progress in experimental techniques for environmental research may also stimulate new approaches in engineering sciences and material inspection.

References

1. O. Breitenstein, W. Warta, and M. Langenkamp, *Lock-in Thermography*, 2nd ed. Springer Berlin Heidelberg, 2010.
2. M. Sackewitz, Ed., *Handbuch zur industriellen Bildverarbeitung*, 3rd ed. Fraunhofer Verlag, 2017.
3. P. Libner, B. Jähne, and E. Plate, "Ein neue Methode zur lokalen und momentanen Bestimmung der Wiederbelüftungsraten von Gewässern," *Wasserwirtschaft*, vol. 77, no. 5, pp. 230–235, 1987.
4. B. Jähne, P. Libner, R. Fischer, T. Billen, and E. J. Plate, "Investigating the transfer process across the free aqueous boundary layer by the controlled flux method," *Tellus*, vol. 41B, no. 2, pp. 177–195, 1989.
5. B. Jähne, L. Warmuth, and K. E. Krall, "Exploring the mechanisms of air-sea gas transfer using thermographic techniques," in *Air-Water Gas Exchange: Cross-linking field measurements, laboratory measurements and modeling*, B. Jähne, K. E. Krall, and C. Marandino, Eds. Heidelberg University Publishing, 2023, in press.
6. J. Kunz and B. Jähne, "Investigating small scale air-sea exchange processes via thermography," *Front. Mech. Eng.*, vol. 4, p. 4, 2018.
7. L. Nagel, K. E. Krall, and B. Jähne, "Measurement of air-sea gas transfer velocities in the Baltic Sea," *Ocean Sci.*, vol. 15, pp. 235–247, 2019.
8. L. Nagel, K. E. Krall, and B. Jähne, "Comparative heat and gas exchange measurements in the Heidelberg Aeolotron, a large annular wind-wave tank," *os*, vol. 11, pp. 111–120, 2015.
9. J. Kunz, "Active Thermography as a Tool for the Estimation of Air-Water Transfer Velocities," Ph.D. dissertation, Institut für Umweltphysik, Fakultät für Physik und Astronomie, Univ. Heidelberg, 2017.
10. L. Warmuth, "Spatio-temporal analysis of air-sea gas transfer with active thermography," Master's thesis, Institut für Umweltphysik, Universität Heidelberg, Germany, 2022.
11. R. Stewing, "Optimierung thermografischer Messmethoden zur Geschwindigkeits- und Geschwindigkeitsgradientenmessung," Bachelor's thesis, Institut für Umweltphysik, Universität Heidelberg, Germany, 2023.
12. M. Bopp, "Luft- und wasserseitige Strömungsverhältnisse im ringförmigen Heidelberger Wind-Wellen-Kanal (Aeolotron)," Master's thesis, Institut für Umweltphysik, Universität Heidelberg, Germany, 2014.